Palladium Sorption on Glutaraldehyde-Crosslinked Chitosan in Fixed-Bed Systems

MONTSERRAT RUIZ,[1] ANA MARIA SASTRE,[2] MARIA CELIA ZIKAN,[3] ERIC GUIBAL[3]

[1] Universitat Politècnica de Catalunya - E.U.P.V.G., Department of Chemical Engineering, Av. Victor Balaguer, s/n., E-08800 Vilanova i la Geltru, Spain

[2] Universitat Politècnica de Catalunya - E.T.S.E.I.B., Department of Chemical Engineering, Diagonal 647, E-08028 Barcelona, Spain

[3] Ecole des Mines d'Alès, Laboratoire Génie de l'Environnement Industriel, 6 avenue de Clavières - F-30319 ALES cedex, France

Received 8 May 2000; accepted 30 August 2000

ABSTRACT: Palladium sorption on glutaraldehyde-crosslinked chitosan was studied in fixed-bed column systems. Sorption performances were controlled mainly by the presence of competitor anions in the solution: The presence of sulfate, chloride, or nitrate (to a lesser extent) significantly decrease sorption properties. Although the influence of other operating conditions such as particle size, column depth, and flow velocity on sorption breakthrough cannot be completely neglected, palladium sorption is less significantly controlled by these parameters than for the sorption of other metal ions, owing to fast mass transfer and weak intraparticle diffusion control. © 2001 John Wiley & Sons, Inc. J Appl Polym Sci 81: 153–165, 2001

Key words: chitosan; palladium; sorption; fixed-bed column; particle size; flow velocity; column depth

INTRODUCTION

Palladium is widely used in industry for the synthesis of catalysts and its high cost may explain the large number of processes focusing on its recovery from dilute aqueous effluents, as well from industrial wastes.[1] Several techniques have been experimented with using adsorption processes, ion-exchange techniques, liquid/liquid extraction, or more sophisticated processes including extractant impregnated resins and liquid membranes.[1–5] However, in facing the technical and/or economical limitations of these processes, there is a need for the development of alternatives processes, especially in the case of dilute effluents. Thus, sorption processes using waste materials have been proposed including fungal biomass[6] or biopolymers.[7,8] Chitosan is one of these new biomaterials which have been screened for metal recovery[9–11] and especially for platinum group metal (PGM) and gold recovery.[8,12–15] Several derivatives of chitosan have been investigated including iminodiacetic acid derivatives[14] or sulfur derivatives[16] for platinum and palladium removal. Since chitosan is soluble in many mineral and organic acids, a crosslinking treatment is frequently used to reinforce the stability of the polymer in acidic solutions.[17] Indeed, due to its cationic behavior in acidic solutions, chitosan is able to sorb metal anions such as molybdate, vanadate, hexachloroplatinate, and tetrachloropalladate through an anion-exchange mechanism be-

Correspondence to: E. Guibal (Eric.Guibal@ema.fr).

Journal of Applied Polymer Science, Vol. 81, 153–165 (2001)
© 2001 John Wiley & Sons, Inc.

tween the counteranions and the metal anions and/or electrostatic attraction between protonated amine groups and metal anions.[8,14] These processes are usually strongly controlled by the presence of competitor anions such as chloride and sulfate, and to limit their influence on sorption performances, chitosan has been modified by grafting new functional groups in order to bring to the ion-exchange resin new chelating functionalities.[16]

Despite the large number of studies on PGM sorption using chitosan, the literature is not really abundant on the optimization of sorption processes regarding sorption isotherms and uptake kinetics. Among the few articles focusing on these investigations, sorption in dynamic systems has rarely been studied. The present study investigated palladium sorption using fixed-bed columns and glutaraldehyde-crosslinked chitosan flakes. Special attention was given to the influence of operating conditions such as flow velocity, metal-ion concentration, column depth, and sorbent particle size. Several models based on fundamental mass-transport mechanisms, including external film, and pore and surface diffusion have been proposed but require the calculation of a number of differential equations.[18–20] In addition, these solutions also require accurate correlations for mass-transfer parameters to describe an external film, internal pore diffusion, and the equilibrium relationship between sorbate and sorbent. There are several simplified design models available such as the bed-depth service time (BDST), derived from the Bohart and Adams equation,[21] the Hutchins approach,[22] and the empty-bed residence time (EBRT).[23] These simplified models are used in this study for the optimization of palladium sorption in small fixed-bed columns before scaling-up of the process.

EXPERIMENTAL

Materials

Chitosan was supplied by ABER-Technologie (Plouvien, France) as a flaked material, with a deacetylation percentage of about 87%, defined by FTIR spectrometry.[11] The mean molecular weight was measured at 125,000, using a size-exclusion chromatography (SEC) method, coupled with a differential refractometer and a multiangle laser light-scattering photometer.[10] The moisture content of sorbent particles, for crosslinked sorbents, was determined at about 10%; sorbent masses are expressed on a wet basis.

Chitosan Crosslinking

Chemical crosslinking of chitosan chains with the bifunctional reagent glutaraldehyde occurs by a Schiff's reaction of aldehyde groups of glutaraldehyde with the amino groups of the chitosan biopolymer chain by formation of imine functions (and water elimination).[24] The glutaraldehyde crosslinking was performed by contacting glutaraldehyde and chitosan flakes for 16 h according to a procedure previously described.[7–8,11,17] The ratio of glutaraldehyde to chitosan (crosslinking ratio CR: mol GA/mol NH_2) was fixed to 1 : 1 Previous investigations on palladium sorption using glutaraldehyde-crosslinked chitosan have shown that it is a good compromise between chitosan stability in acidic solutions and chitosan reactivity (remaining free amine groups and crystallinity). The crosslinked chitosan particles were extensively rinsed with demineralized water.

This general procedure was applied to the crosslinking of chitosan flakes, of which the original particle sizes were $G1 < 125 < G2 < 250 < G3 < 500 < G4 < 710$ μm. The size of the initial particles was not changed by the crosslinking step. Dissolution testing in sulfuric acidic solutions (pH ca. 3) has shown that chitosan does not significantly dissolve after the crosslinking step: The chitosan concentration in the solution was measured using the acid red titration method,[24] and it was found that the dissolving of chitosan does not exceed 1%. These findings demonstrate that the crosslinking is stable in our experimental conditions. A pycnometric measurement of the density of the crosslinked flakes showed that the density is almost constant for each of the size fractions and the crosslinking ratio. The mean value, calculated on nine samples, was found to be 1.36 kg L^{-1}.

Experimental Procedure for Palladium Sorption

Palladium solutions were prepared from palladium chloride ($PdCl_2$, ChemPur) in demineralized water (except in studies of the influence of chloride, sulfate, and nitrate ions, which were added in the form of NaCl, Na_2SO_4, and $NaNO_3$, respectively). Alternatively, for duplicate experiments, palladium solutions were prepared from ammonium tetrachloropalladate [$(NH_4)_2PdCl_4$, ChemPur], and experiments have confirmed that palla-

dium is not influenced by the kind of palladium salt. The pH of the solutions was controlled using either hydrochloric acid or sulfuric acid and sodium hydroxide concentrated solutions (5*M*). The pH was kept constant during the sorption step.

For sorption isotherms, known volumes of palladium solutions (100 mL) at fixed concentrations (10, 20, or 40 mg L^{-1}) were put into contact with varying sorbent quantities (ranging from 5 to 30 mg wet mass) at room temperature (20 ± 1°C). After 3 days of agitation, in a reciprocal shaker, solutions were filtered through 1.2-μm filtration membranes and the filtrates were analyzed using the $SnCl_2$/HCl spectrophotometric method (using a Shimadzu 1601 UV-visible spectrophotometer, Japan) or, alternatively, using ICP analysis (Jobin-Yvon JY36, France).[25] Control experiments showed that no sorption occurred on either the glassware or filtration systems. The sorption capacity, or palladium concentration in the sorbent, was obtained using a mass-balance equation and was expressed as mg Pd g^{-1} sorbent, without reference to actual chitosan content in the sorbent, which is, in turn, dependent on the crosslinking ratio.

For the study of sorption kinetics, a standard procedure was applied.[11] One liter of a palladium solution at a fixed pH was mixed with a fixed mass of sorbent in a jar-test agitated system (240 rotations per minute). Five-milliliter samples were withdrawn at specified times and filtered through a 1.2-μm filtration membrane and analyzed as previously specified.

For the study of sorption in continuous systems, a column (internal diameter: 7 mm) was filled with differing amounts of the sorbent and was fed with an acidic solution of palladium (pH 2) with different flow rates. Samples were regularly collected and analyzed. Randomly, some breakthrough curves were duplicated, proving that experiments are reproducible (within an error lower than 8% in the breakthrough volume and with a similar breakthrough slope).

Empirical Modeling of Breakthrough Curves

The breakthrough curves were drawn as a function of the bed volumes (BVs) passed through the column (volume passed through the column divided by the volume of the column—based on the empty-bed column volume) V_c (m^3); $V_c = Z\,S$, where Z is the column depth (m), and S, the cross-section area of the column (m^2), taking into account the differences in column height brought about by the change in particle size (G2, G3). The experimental data were mathematically matched to the following equation:

$$\frac{C(t)}{C_0} = \frac{1}{1 + \exp[-\alpha(\mathrm{BV} - \mathrm{BV}_0)]} \tag{1}$$

where BV_0 and α are the parameters to be determined. They were determined using a nonlinear regression analysis (the Levenberg–Marquardt algorithm included in Mathematica® software). BV_0 represents the virtual volume of the solution for which the outlet concentration reaches 50% of the inlet concentration. Assuming the breakthrough curve to be symmetrical around the point (BV_0, 0.5), BV_0 could be theoretically correlated with the concentration of the sorbate C_0, the amount of the sorbent in the volume V_c, m, and the sorption capacity $q(C_0)$ (determined from the sorption isotherms and corresponding to the sorption capacity at the equilibrium concentration equal to the inlet concentration) according to

$$\mathrm{BV}_0 C_0 V_c = m q(C_0) \tag{2}$$

Equation (1) may be transformed to

$$\mathrm{BV} = \mathrm{BV}_0 - \frac{1}{\alpha}\ln\left(\frac{C_0}{C(t)} - 1\right) = \frac{U_0 t}{Z} = \frac{v\varepsilon t}{Z} \tag{3}$$

where U_0 is the superficial flow velocity ($U_0 = Q/S$), Q is the flow rate ($m^3\ h^{-1}$), ν represents the linear flow velocity or the interstitial flow velocity ($m\ h^{-1}$), $\nu = U_0/\varepsilon$, and ε is the column voidage (the column voidage with this flake shape of particules was found to vary from 0.73 to 0.79, the average value was used for calculations: 0.76 in the case of G2 particles, 0.86 for G3 particles).

This equation is similar to those derived from the Bohart and Adams model [20] which gives

$$t = \frac{N_0 Z}{C_0 v} - \frac{1}{kC_0}\ln\left[\frac{C_0}{C(t)} - 1\right] = sZ - s_0 \tag{4}$$

$$\ln\left[\frac{C_0}{C(t)} - 1\right] = \ln\left[\exp\left(\frac{kN_0 Z}{v}\right) - 1\right] - kC_0 t \tag{5}$$

where N_0 is the volumetric sorption capacity (kg m^{-3}), which is equal to $q(C_0)(1 - \varepsilon)\rho/\varepsilon$; ρ represents the sorbent volumetric mass (kg m^{-3}). The kinetic constant is represented by k ($m^3\ kg^{-1}\ h^{-1}$). The critical bed depth Z_0 is obtained for t

= 0 and for a fixed outlet concentration $C(t) = C_b$ (C_b is the concentration at the breakthrough defined as a limit concentration or a fixed percentage of the inlet concentration):

$$Z_0 = \frac{v}{kN_0} \ln\left[\frac{C_0}{C(t)} - 1\right] = \frac{v}{kN_0} \ln\left(\frac{C_0}{C_b} - 1\right) \quad (6)$$

The critical bed depth represents the theoretical depth of the sorbent necessary to prevent the sorbate concentration from exceeding the limit concentration C_b. Another important parameter is the coefficient s_0, defined using the Hutchins equation [derived from eq. (4)].[22] It represents the time required for the adsorption wave front to pass through the critical bed depth. It is obtained from

$$s_0 = \frac{1}{kC_0} \ln\left(\frac{C_0}{C_b} - 1\right) \quad (7)$$

The coefficient s is the slope of eq. (4); it represents the time required to exhaust a unit length of the column under the selected experimental conditions and with the limit outlet concentration:

$$s = \frac{N_0}{C_0 v} \quad (8)$$

RESULTS AND DISCUSSION

Palladium Sorption on Glutaraldehyde-crosslinked Chitosan: Isotherms and Kinetics in Batch Systems

Figure 1 presents palladium-sorption isotherms for different particle sizes of the sorbent at pH 2.

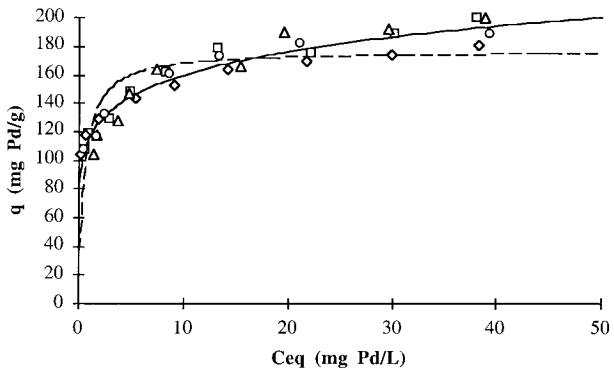

Figure 1 Influence of particle size on palladium-sorption isotherms at pH 2 (pH controlled with HCl: (□) G1; (◇) G2; (△) G3; (○) G4; (solid line) Freundlich model and (dashed line) Langmuir model for joined series.

Experimental data can be described by either the Langmuir equation or the Freundlich equation:

$$\text{Langmuir equation} \qquad q = \frac{q_m b C_{eq}}{1 + bC_{eq}} \quad (9)$$

$$\text{Freundlich equation} \qquad q = k_F C_{eq}^{1/n} \quad (10)$$

where q (mg g^{-1} or mmol g^{-1}) and C_{eq} (mg L^{-1} or mmol L^{-1}) represent the concentration at equilibrium in the solid and the liquid phases, respectively; q_m is the maximum sorption capacity at saturation of the monolayer (mg g^{-1} or mmol g^{-1}), and b, the ratio of sorption-to-desorption rates (L mg^{-1} or L $mmol^{-1}$). k_F ($mg^{1-1/n}$ g^{-1} $L^{-1/n}$) and n are the parameters of the Freundlich model.

Table I presents the values of the Langmuir and the Freundlich model parameters for palla-

Table I Parameters of the Langmuir and Freundlich Models for Palladium Sorption Using Glutaraldehyde-Crosslinked Chitosan with Varying Particle Size at pH 2 (pH Controlled with HCl)

	Langmuir Model			Freundlich Model		
Particle Size	q_m (mg g^{-1})	b (L mg^{-1})	MSR	k ($mg^{1-1/n}$ g^{-1} $L^{-1/n}$)	n	MSR
G1	181.3	1.86	13.72	117.1	6.98	5.18
G2	162.6	5.59	11.04	122.1	9.76	4.17
G3	196.9	0.70	9.11	105.9	5.55	6.96
G4	179.7	1.66	13.02	115.0	6.90	4.81
Joined series	177.1	1.90	16.57	115.6	7.09	7.51

MSR: mean sum residuals according to MSR = $\sqrt{[\Sigma_{i=1}^{n} (F_{exp}(C_i) - F_{calcd}(C_i))^2]/n}$, with F the function representative of the sorption equation (Langmuir or Freundlich equation).

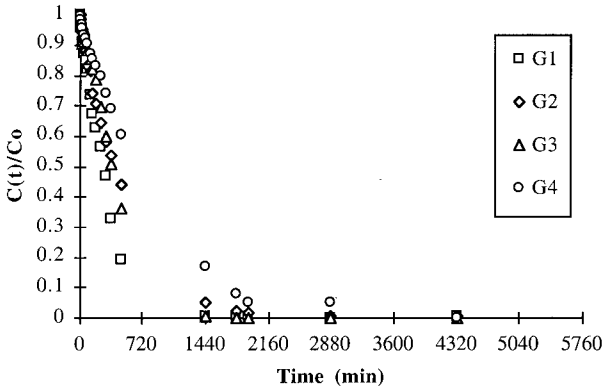

Figure 2 Influence of sorbent particle size on palladium-sorption kinetics at pH 2 (controlled with HCl; C_0: 20 mg Pd L^{-1}; SD: 100 mg L^{-1}).

dium sorption on glutaraldehyde-crosslinked chitosan for different particle sizes of the sorbent. The MSR coefficient shows that the Freundlich model fits the experimental data better than does the Langmuir equation.

Moreover, it appears that the particle size hardly influences the sorption isotherms: Sorption capacity is not influenced by the diameter of the sorbent particles. This finding contrasts with previous results on the sorption of uranium using chitosan flakes[26] and the extraction of molybdate with crosslinked chitosan flakes.[27] In the latter cases, the diffusion of polynuclear ions of large ionic size is sterically hindered by the low porosity of chitosan, and sorption is restricted to the external layers of the biopolymer. A chitosan gel conditioning may reduce this hindering effect.[11] The weak effect of the particle size on the sorption capacity is an important characteristic for the design of fixed-bed systems: The volumetric capacity of the columns will only be changed by a change in the void fraction of the column when the particle size is increased.

Another important characteristic of these sorption isotherms appears in the shape of the curves: Palladium sorption on glutaraldehyde-crosslinked chitosan is very favorable. The sorption capacity increases strongly at a low residual concentration and reaches a quasi-plateau: Sorption capacity will not be significantly changed above a 10-mg L^{-1} residual palladium concentration.

Figure 2 presents the influence of the particle size on palladium-sorption kinetics. Although an increasing particle size increases the time required to reach equilibrium, the influence of this parameter is not very strong in comparison to the sorption of other metal anions (such as molybdate and vanadate) on similar sorbents.[11] The sorption of metal ions may be controlled by their diffusion in the polymer network. Since chitosan is a material of low porosity, increasing the size of the sorbent particle size limits mass transfer of large molecules such as polynuclear hydrolyzed molybdate, while the diffusion of mononuclear species such as hexachloroplatinate and tetrachloropalladate anions is hardly influenced.[8] Owing to the weak effect of the particle size on the sorption kinetics in batch systems, this parameter is supposed to hardly affect the breakthrough curves; however, particle size may influence the external diffusion coefficient in a fixed-bed column. Sorption kinetics are more significantly affected by the metal concentration as shown on Figure 3. Increasing the initial concentration significantly increases the time required to reach equilibrium; the slope of the decay curves decreases with high metal concentrations [Fig. 3(a)]. It may vary the depth of the sorption zone and then influence the slope of the breakthrough curves. However, Figure 3(b) shows that the sorption rate (amount of

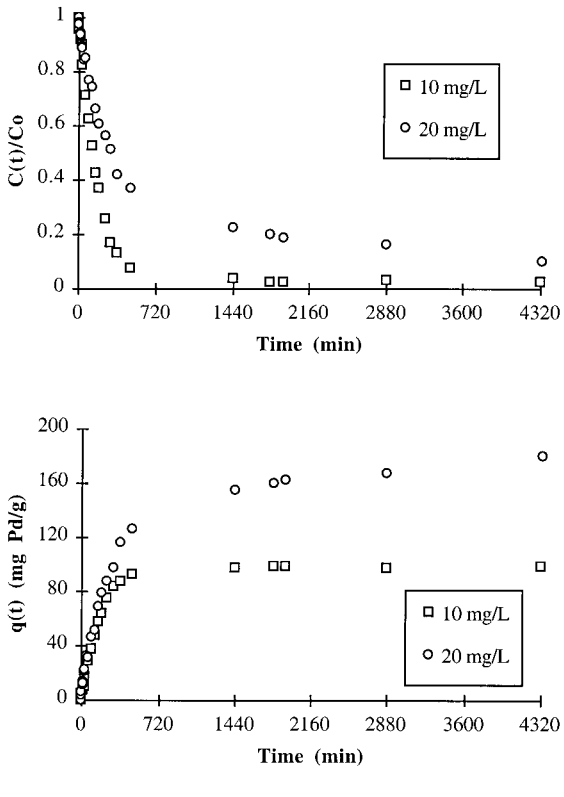

Figure 3 Influence of palladium concentration on sorption kinetics at pH 2 (controlled with hydrochloric acid; SD: 100 mg L^{-1}).

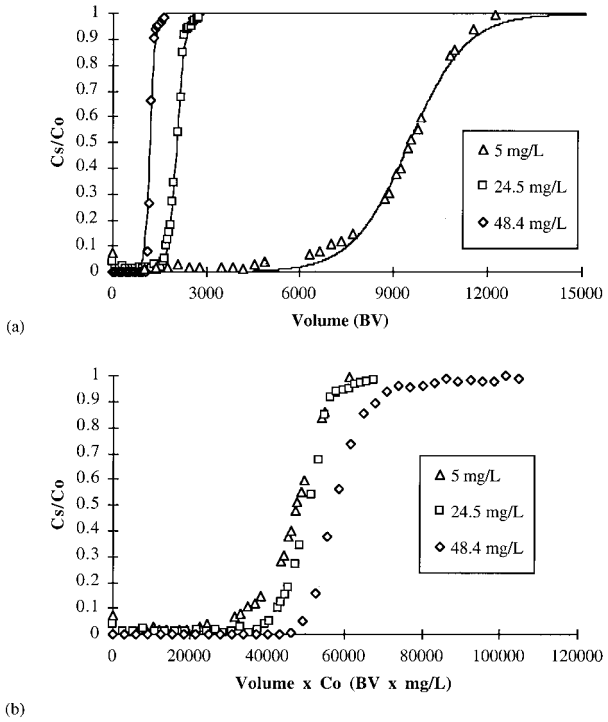

Figure 4 Influence of initial concentration on palladium-sorption breakthrough curves.

palladium adsorbed on the solid) increases with the initial concentration.

Influence of Palladium Concentration on Breakthrough Curves

Figure 4(a) shows the influence of inlet palladium concentration on the breakthrough curves. As expected, increasing the metal concentration reduces the breakthrough volume significantly; however, this reduction is not proportional to that of the metal concentration: It seems that increasing the metal concentration makes the system more efficient. Figure 4(b) shows the same curves with a different x-axis (the volume—in BVs—times the initial concentration): It confirms that an increasing metal concentration increases the amount of metal to be treated by the sorbent before the breakthrough. The difference is not so significant when the exhaustion points are compared [Fig. 4(b)]. Moreover, as expected, with increasing metal concentration, the slope of the breakthrough curves increases, indicating a better mass transfer in the column. Palladium concentration at the column exhaustion increases with the initial concentration, reaching 150, 178, and 198 mg g^{-1} for 5, 25, and 50 mg L^{-1}, respectively. These values are close to those obtained for the sorption isotherms: 155, 170, and 182 mg g^{-1}, respectively. Table II shows the modeling of the breakthrough curves with the empirical eq. (1); the coefficient α increases with the concentration. This coefficient may be related to the slope of the breakthrough curve at the half-exhaustion point [$C(t) = 0.5\ C_0$] according to the equation

$$\left[\frac{d\left(\frac{C(\mathrm{BV})}{C_0}\right)}{d\mathrm{BV}}\right]_{\mathrm{BV}=\mathrm{BV}_0} = \frac{\alpha}{4} \qquad (11)$$

Table II confirms that the slope of the curve increases with the inlet concentration; the coeffi-

Table II Influence of Experimental Conditions on the Parameters of the Empirical Modeling of Breakthrough Curves [Eq. (1)]

Experiment Run	C_0 (mg L^{-1})	U_0 (m h^{-1})	Z (cm)	d_c (mm)	d_p (μm)	Competitor Ion (M)	BV^0	$\alpha \times 10^3$
1	5	0.65	4.5	7	125–250	—	9498	1.11
2	25	0.65	4.5	7	125–250	—	2049	7.69
3	50	0.65	4.5	7	125–250	—	1194	13.11
4	50	0.37	4.5	7	125–250	—	1160	14.13
5	50	1.57	4.5	7	125–250	—	1157	13.55
6	50	0.65	2.4	7	125–250	—	1069	12.50
7	50	0.65	6.6	7	125–250	—	1204	15.94
8	50	0.65	2.3	10	125–250	—	1079	12.14
9	50	0.65	6.7	7	250–500	—	884	20.47
10	50	0.65	4.5	7	125–250	0.1 Cl^-	816	18.10
11	50	0.65	4.5	7	125–250	0.2 NO_3^-	980	9.87
12	50	0.65	4.5	7	125–250	0.1 SO_4^{2-}	516	14.48

Table III Influence of Experimental Conditions on the Parameters of the Bohart–Adams and Hutchins Models

Experiment Run	Z_0 (cm)	s (h m^{-1})	s_0 (h)	N_0 (kg m^{-3})	k (m^3 kg^{-1} h^{-1})
1	1.26	14,613	183.5	62.49	3.21
2	0.84	3152	26.5	67.40	4.45
3	0.85	1837	15.5	78.55	3.79
4	0.81	3134	25.4	76.28	2.32
5	0.84	737	6.2	76.14	9.46
6	0.53	1645	8.7	70.36	6.77
7	1.01	1853	18.7	79.24	3.14
8	0.52	1659	8.6	70.96	6.86
9	1.09	557	14.8	21.04	3.97
10	0.90	1255	11.3	53.66	5.23
11	1.37	1508	20.7	64.47	2.85
12	1.78	794	14.1	33.94	4.18

cient α varies as a power function of the initial concentration according to the following equation which may be considered as an indicative trend (only three different initial concentrations have been tested):

$$\alpha = 1.211 \times 10^{-4} C_0^{1.349} \qquad (R^2 = 0.989) \quad (12)$$

Table III presents the standard Bohart and Adams–Hutchins coefficients of the BDST model calculated from eqs. (4)–(8) and deduced from the modeling of the breakthrough curves using eq. (1). The kinetic parameter, k, does not vary continuously with the concentration. No explanation has been found for this trend. As expected, increasing the inlet concentration increases the volumetric capacity of the sorbent in the column from 62 to 79 g L^{-1}. These values may be converted to sorption capacities using the apparent volumetric mass of the sorbent in the column (and the mass of sorbent used for each experiment): Dynamic sorption capacities range from 160 and 200 mg g^{-1}, values close to those obtained in batch systems. The volumetric capacity N_0 varies almost linearly with the concentration following this indicative equation:

$$N_0 = 59.87 + 360.5 C_0 \qquad (R^2 = 0.976) \quad (13)$$

The breakthrough time is defined as the time required to reach an outlet concentration representing 5% of the inlet concentration, while the exhaustion point is defined as the time when the outlet concentration reaches 95% of the inlet concentration. The critical bed length of the column decreases when the concentration increases from 5 and 25 mg L^{-1}, after which it stabilizes. On the other hand, as expected, the time required to exhaust a unit length of the sorbent in the column (s) under the test conditions continuously decreases with an increasing initial concentration. The time required for the adsorption wave front to pass through the critical bed depth (s_0) varies with the reciprocal of the inlet metal concentration.

An increasing metal concentration progressively increases the degree of sorbent usage (DoSU), defined as the ratio of the metal sorbed at the breakthrough to the metal adsorbed as the exhaustion point of the column (Table IV). The sorbent usage rate (sorbent mass used at the breakthrough volume) varies linearly with the concentration, according the following equation:

$$\mathrm{SUR} = 33.11 \times 10^{-3} + 5.308 C_0 \qquad (R^2 = 0.995) \quad (14)$$

Thus, it is possible to easily manage the change of column systems under experimental conditions corresponding to a constant feed concentration.

Influence of Superficial Flow Velocity on Breakthrough Curves

Figure 5 shows the effect of the superficial velocity on the palladium-sorption breakthrough curves. The influence of this parameter is almost negligible. Chase discussed the influence of the usual

Table IV Influence of Experimental Conditions on Sorbent Usage Rate (SUR: g L^{-1}, Sorbent Mass/Breakthrough Volume) and Degree of Sorbent Usage (DoSU: %, Palladium Mass Sorbed at Breakthrough/Mass Sorbed at Exhaustion)

Experiment Run	EBCT (min)	V_{brk} (mL)	V_{exh} (mL)	q_{brk} (mg g^{-1})	q_{exh} (mg g^{-1})	SUR (g L^{-1})	DoSU (%)
1	4.15	9183	19,920	87.9	150.7	0.054	58
2	4.15	2843	4261	137.0	177.4	0.176	77
3	4.15	1699	2683	164.0	198.2	0.294	83
4	7.30	1586	2191	157.0	190.4	0.315	82
5	1.72	1587	2275	151.9	184.0	0.315	83
6	2.22	775	1069	185.1	213.0	0.323	87
7	6.09	2547	3479	164.9	197.6	0.294	83
8	2.12	1507	2356	137.2	176.5	0.332	78
9	6.18	1913	2610	185.4	208.5	0.261	89
10	4.15	1095	1597	102.5	129.2	0.457	79
11	4.15	1274	2537	125.2	165.0	0.392	76
12	4.15	667	1764	63.2	91.7	0.750	69

operating parameters on the shape of the breakthrough curves and observed that the flow velocity has no significant effect on the position and the shape of the curves when the reciprocal of coefficient b of the Langmuir equation is negligible compared to the inlet concentration.[28] Although the sorption isotherms are more accurately described by the Freundlich equation, we will use this criterion to evaluate the influence of this parameter. The criterion proposed by Chase is satisfied here, and it explains the weak effect of flow velocity.

The overlapping of the breakthrough curves indicates that mass transfer in fixed-bed columns is not controlled by the superficial velocity under the selected experimental conditions (in this velocity range). The slight variations may be due to experimental inaccuracies rather than to a difference in the mass transfer. The empty-bed contact time (EBCT) is given in Table IV, and for this experimental series, the EBCT varies between 1.7 and 7.3 min. By taking into account the voidage of the column (ε: 0.76—experiments performed with G2 particles) the mean residence time varies from 1.3 to 5.6 min. In spite of such a short residence time, the sorption is very efficient and weakly affected by the flow velocity. This result may be related to the fast sorption kinetics obtained in batch systems (Figs. 2 and 3): Sorption rates are significantly higher than are those observed, for example, with molybdate. Consequently, palladium-sorption breakthrough curves were less affected by the flow rate in the column than were those for molybdate using similar sorbents.[29,30]

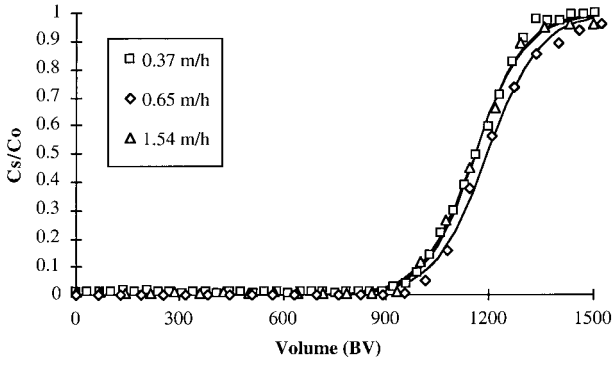

Figure 5 Influence of superficial velocity on palladium-sorption breakthrough curves.

BV_0 and α are almost unchanged with an increasing superficial flow velocity (Table II): The variation does not exceed 5 %. The coefficient, α, increases slightly by decreasing the flow velocity. However, the slope of the linear part of the breakthrough curves is not so strongly affected by the flow velocity, as it was for molybdate sorption.[29,30] The sorption capacity varies, but in the same order of magnitude. This finding is consistent with the conclusions of a previous study of McKay et al. on dye binding using chitin in dynamic systems.[31] Kast and Otten showed that in the case of a favorable isotherm (concave isotherms such as encountered with Langmuir-type isotherms) the slope of the curve becomes progressively steeper as the favorability of the isotherm

increases.[32] In the case of palladium sorption, the Freundlich equation fits the experimental sorption isotherm well and the sorption is very favorable (steep curve at low residual concentrations). The kinetic coefficient varies with the superficial flow velocity according to the equation

$$k = 7.37 \times 10^{-3} + 6.003U_0 \qquad (R^2 = 0.999) \tag{15}$$

The kinetic coefficient, k, depends on the effect of both external and intraparticle diffusion.[23] While the external diffusion is controlled by the flow velocity (this control may be predicted using well-known correlations such as the one proposed by Williamson[33]), intraparticle diffusion is not affected by the flow rate. The dependence of the rate parameter with the flow velocity indicates that both mechanisms are rate-controlling.[23] The occurrence of several intraparticle diffusion mechanisms, including pore and surface diffusion, makes the discussion of the influence of diffusion mechanisms on the shape of the breakthrough curves very difficult. Ma et al.[34] concluded that the shape of the curve depends on the predominance of pore or surface diffusion, which, in turn, depends on both the type of the sorption isotherm that describes the equilibrium and the solute concentration.

The SUR and the DoSU do not significantly change with the superficial velocity under current experimental conditions: SUR varies between 0.294 and 0.315 kg m^{-3} and the DoSU is in the range 82–83 %. It makes the fixed-bed system easy to manage: The change of the exhausted column may readily be predicted.

Influence of Column Depth (Sorbent Amount) on Breakthrough Curves

Increasing the column depth is expected to affect the volume of the solution corresponding to an outlet concentration of 50% of the inlet concentration[23]; however, reporting the breakthrough curves as a function of the BV allows the influence of the geometry of the column to be reduced, and similar breakthrough curves would be expected. The BV of the solution for half-exhaustion ($C_s/C_0 = 0.5$) would be expected to be almost identical for different amounts of sorbents (and different column depth), while the slope of the breakthrough curves would change with the column depth: Increasing the depth of the column increases the contact time between the sorbent and the sorbate. In the case of low porous sorbents for which the intraparticle diffusion is the rate-limiting step, it would strongly affect the breakthrough curves. In the case of palladium uptake, the sorption process is considered to be less affected by intraparticle diffusion than that of large polynuclear hydrolyzed species (in the case of molybdate). In this study, palladium diffusion is not really sterically hindered. For differing column depths (2.4, 4.5, and 6.6 cm), the sorption capacities at exhaustion are comparable (from 195 to 199 mg g^{-1}). However, with a short column, the breakthrough occurs at a lower BV number and the slope of the curve is reduced: Increasing column depth increases the EBCT from 2 to 6 min and the residence time from 1.5 to 4.6 min. The differences are not very marked, certainly as a consequence of the very efficient mass transfer of palladium in sorbent flakes. This result contrasts with the strong effect of the column depth on breakthrough curves obtained for uranium sorption using chitosan flakes[35]: In the case of uranium sorption, intraparticle diffusion is considered a limiting step in the sorption process.

Increasing the depth of the column involves small variations in the parameters of the models (Tables II–IV): N_0, BV_0, and α slightly increase, while k, DoSU, and SUR slightly decrease. However, the variations are significantly lower than in changing the flow velocity and the inlet concentration of palladium. The most significant differences are observed for the shortest column size. The critical bed depth progressively increases with the depth of the column; however, Z_0 represents a decreasing fraction of the total column depth when increasing this parameter: 22, 19, and 15% for 2.4-, 4.5-, and 6.6-cm-long columns, respectively.

Influence of Column Diameter on Breakthrough Curves

Experiments were performed with a differing column diameter. Figure 6 shows three breakthrough curves obtained with the same column depth (10 mm– 2.3 cm, and 7 mm– 2.4 cm) and with the same amount of sorbent (10 mm–2.3 cm and 7 mm–4.5 cm) with the same superficial flow velocity. Comparison of these three curves makes it possible to detect and separate the respective influence of column depth and column diameter. The change in the column diameter does not change the breakthrough curves (neither BV_0 nor α) for a similar column depth. For comparable

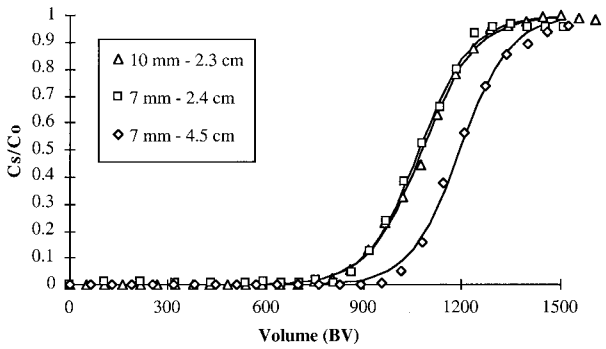

Figure 6 Influence of column diameter on palladium-sorption breakthrough curves.

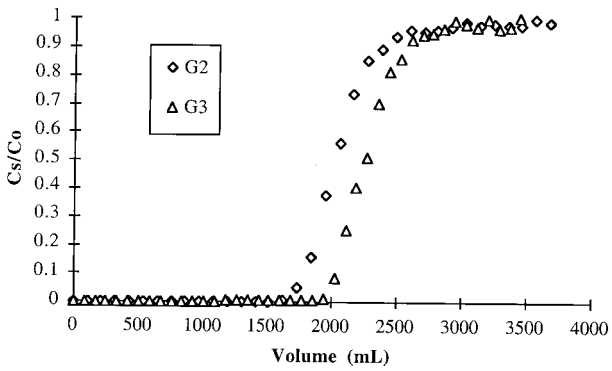

Figure 8 Influence of sorbent particle size on palladium-sorption breakthrough curves.

sorbent amounts (10 mm–2.3 cm, and 7 mm–4.5 cm), the lowest column depth used for the experiment with a column diameter of 10 mm is less favorable to sorption, perhaps due to a contact time too brief and dispersion effects. This finding is consistent with previous results on the effect of column depth (Fig. 7). For the same amount of sorbent, enlarging the column results in a diminution of column depth. As a consequence, the resistance to diffusion may limit the overall mass transfer and the sorption efficiency.

Influence of Sorbent Particle Size on Breakthrough Curves

Kast and Otten showed that in the case of a favorable isotherm (i.e., a concave isotherm as with Langmuir-type isotherms) the slope of the curve becomes progressively steeper as the favorability of the isotherm increases.[32] In the case of palladium sorption, the Freundlich equation fits the experimental sorption isotherm well, and the sorption is very favorable (steep curve at low residual concentrations). Sorption isotherms are not really affected by the sorbent particle size and the curves overlap. In these conditions, this experimental parameter is assumed to be nonlimiting. Surprisingly, Figure 8 shows that increasing the size of sorbent particles reduces the sorption performance (a greater volume at breakthrough and at exhaustion of the column). One would expect a reciprocal trend: Increasing the sorbent particle size usually limits mass transfer. No explanation of this experimental result, which was obtained several times, has yet been found. The figure presents breakthrough curves for G2 and G3 particles with their actual depth in the 7-mm-diameter columns for a sorbent mass of 0.5 g (4.5 cm for G2 fraction and 6.7 cm for the G3 fraction). The voidage fraction in the column increases with the size of the sorbent flakes from 76 to 86% for the G2 and G3 fractions, respectively. This finding could explain this unexpected trend.

Sorption capacity is also increased. These results contrast with those from the sorption isotherms in batch systems. Sorbent particle size may influence the sorption kinetics (Fig. 2) but not the equilibrium. In these conditions, we could expect a similar 50% breakthrough point (comparable to BV_0), but a lower breakthrough slope. A reverse trend is observed in the experimental data: Breakthrough slopes are comparable while the breakthrough volume at 50% of the inlet concentration is significantly lower for the largest particles. Surprisingly, using the G3 size fraction leads to a higher DoSU and a lower SUR, compared to the G2 fraction (Table IV). The kinetic coefficient k and the time required for the adsorption zone to pass through the critical bed depth are not significantly affected by the size of the particle (Table III). The critical bed depth is in-

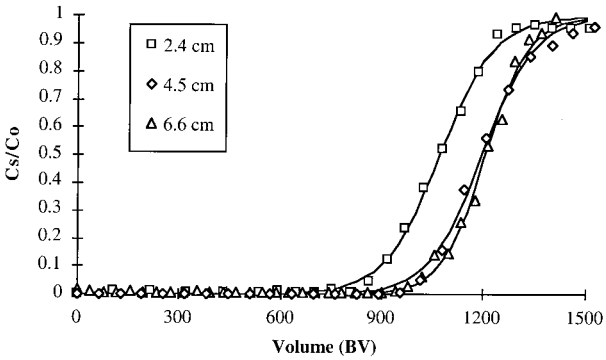

Figure 7 Influence of column depth on palladium-sorption breakthrough curves.

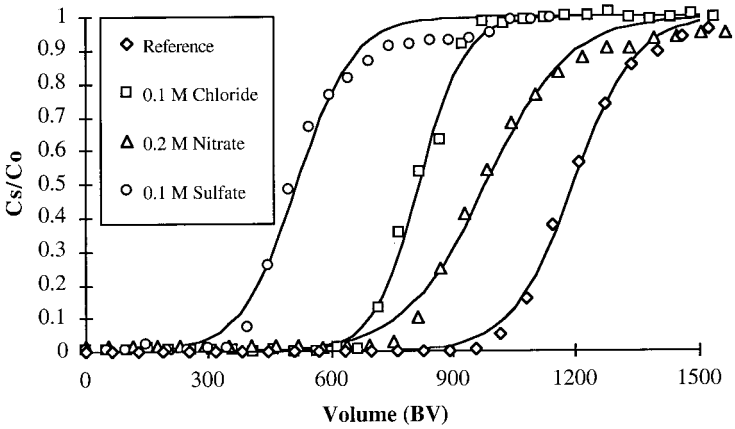

Figure 9 Influence of competitor ions on palladium-sorption breakthrough curves.

creased by 15%, but it represents only 16% of the total depth of the column. As expected, increasing the size of the sorbent induces a strong decrease in the volumetric sorption capacity; however, the variation is not proportional to the volume variation of the column (V_c). The time required to exhaust a unit length of the sorbent is also strongly decreased. Ko et al. studied the effect of the particle size on breakthrough curves for metal-ion sorption on bone char sorbents.[23] They attributed the increase in the sorption performance level when decreasing the size of the sorbent particles to diffusion restrictions. They underline the effect of increasing the particle size on the increase of the column depth to partly explain these results. The discrepancies between the experimental data and the predictions from the Hutchins' and Bohart–Adams' models has also been attributed to the fact that the basic hypothesis of these models is not verified in these systems (ca. a rectangular sorption isotherm).[23] The influence of this parameter is not restricted to diffusion properties. It may affect the pressure drop inside the column, which can be calculated using the Ergun equation:

$$\frac{dP}{dZ} = \frac{v(1-\varepsilon)}{d_p\varepsilon^3}\left(\frac{150(1-\varepsilon)\mu}{d_p} + 1.75\rho_l v\right) \quad (16)$$

where μ and ρ_l are the viscosity (N s m^{-2}) and the volumetric mass of the solution (kg m^{-3}), respectively. Increasing the particle size of the sorbent may result in a significant drop in pressure in the column. The optimization of the process should take into account both hydraulic and mass-transfer properties, and it seems preferable to avoid using the smallest-size fraction (G1: 0.125 μm). The permeability coefficient was shown to vary from 1.4×10^{-12} m^2 and 17×10^{-12} m^2 under comparable experimental conditions.[35] In the case of uranium sorption, the influence of particle size on the kinetics in both batch and columns systems was more marked, due to intraparticle diffusion limitations.[26,35]

Influence of Competitor Ions on Breakthrough Curves

The presence of competitor anions involves a strong decrease in palladium-sorption performance.[7] The sorption mechanism is assumed to be an anion-exchange process involving the exchange of the counterion near the protonated amine groups or the electrostatic attraction of metal anions to these protonated amine groups. The presence of competitor anions reduces the number of amine groups available for palladium sorption. Figure 9 shows the breakthrough curves for palladium sorption on glutaraldehyde-crosslinked chitosan flakes at pH 2, in the presence of chloride, nitrate, and sulfate anions, using standard experimental conditions: inlet concentration 50 mg L^{-1}; sorbent mass: 0.5 g; column depth: 4.5 cm; and superficial flow velocity: 0.65 m h^{-1}. The influence of these anions is very strong but depends on the kind of anions.

Considering the volume at 50% of the exhaustion (BV_0), the competitor effect may be clearly classified following the sequence sulfate > chloride > nitrate. Similar observations on the influence of competitor anions have been cited for platinum sorption using glutaraldehyde-crosslinked

chitosan.[8] It is interesting to note that in spite of the nitrate concentration, which is twice that of chloride, the breakthrough volume in the presence of nitrate is significantly higher than that obtained in the presence of chloride. The sulfate interaction is significantly stronger than that of chloride. This effect has been correlated to their differences in the ionic radius and the ionic charge and also to the different behaviors of these ions in the presence of palladium: Palladium may react with chloride to form anionic species which are adsorbable, while sulfate anions do not interact with palladium. The speciation of palladium strongly depends on the pH, total metal concentration, and chloride concentration: In the presence of sulfate anions instead of chloride anions (brought by sulfuric acid rather than hydrochloric acid for pH control), chloride concentration is not sufficient to form a number of adsorbable palladium species and the sorption efficiency decreases. To avoid such interferences or decrease their influence of platinum/palladium sorption, chitosan has been modified by grafting new functional groups including sulfur moieties (thiourea, rubeanic acid).[16]

The slope of the breakthrough curves is similar for each curve with the exception of that obtained in the presence of nitrate: In this case, the slope is steeper. The sorption capacity is greater but the mass transfer is more affected by the presence of nitrate. It is difficult to find an explanation for this result. The presence of competitor ions involves a significant variation in the model parameters (Tables II–IV): (a) The critical bed depth, Z_0, and the sorbent usage rate, SUR, are significantly increased; (b) the volumetric capacity, N_0, the degree of sorbent usage at breakthrough, DoSU, and the time required to exhaust a unit of length of sorbent, s, are decreased; the kinetic coefficient, k, and the time required for the adsorption zone to pass through the critical bed depth, s_0, remains at the same order of magnitude. The presence of competitor ions affects mainly equilibrium parameters more than kinetic parameters.

It is important to observe that sorption performance levels in the dynamic systems investigated in this study are controlled more by the presence of competitor ions than by the parameters related to mass transfer (diffusion and hydraulic). This finding may be explained by the relatively fast mass transfer of chloropalladate species in these sorbents in comparison to other metal–chitosan systems, for which the control of mass transfer by diffusion properties is such that the hydraulic parameters control the sorption breakthrough curves owing to their influence on the residence time and, consequently, on the mass-transfer resistance in the columns.

CONCLUSIONS

Glutaraldehyde-crosslinked chitosan flakes are very efficient at removing palladium from dilute solutions. Sorption capacities as high as 190–200 mg g^{-1} have been obtained in batch systems. The same sorption levels are reached with fixed-bed column systems. Owing to the relative fast sorption kinetics obtained in palladium sorption with these sorbents (in batch systems), it is not suprising to obtain favorable sorption breakthrough curves: The curves are characterized by steep slopes.

The breakthrough curves are controlled by several experimental parameters such as the column depth, the superficial flow velocity, the metal concentration, and also the size of the sorbent particles. However, although the effect of these parameters cannot be neglected, the differences are not so marked as with other sorbent/sorbate systems. In the case of molybdate sorption, using chitosan gel beads, the influence of intraparticle diffusion on the kinetic control is more marked and the breakthrough curves are more sensitive to the variation in the hydrodynamic parameters (flow velocity, column depth, etc.) and the sorbent parameters (particle size, conditioning, etc.). In the case of palladium, the ready diffusion of mononuclear metal species is not sterically hindered as with systems involving the diffusion of polynuclear hydrolyzed species (molybdate, vanadate).

The influence of competitor anions is more significant: A strong reduction in the volume of the solution which can be recovered with a fixed amount of sorbent is significantly reduced: A 0.1 molar solution of sulfate is sufficient to reduce the half-exhaustion volume (BV_0) from 1150–1200 BV to 450 BV. This competitor effect may be significantly decreased by using modified chitosan obtained by grafting sulfur derivatives on a chitosan backbone: This modification of chitosan brings to the anion-exchange resin new chelating functionalities: It makes the sorbent less sensitive to the ionic strength and to the presence of competitor anions.

REFERENCES

1. Brooks, C. S. Metal Recovery from Industrial Wastes; Lewis: Chelsea, MI, 1991.

2. Beauvais, R. A.; Alexandratos, S. D. React Funct Polym 1998, 36, 113–123.
3. Cortina, J .L.; Miralles, N.; Aguilar, M.; Sastre, A. M. Hydrometallurgy 1996, 40, 195–206.
4. Fu, J.; Nakamura, S.; Akiba, K. Sep Sci Technol 1997, 32, 1433–1445.
5. Fontas, C.; Salvado, V.; Hidalgo, M. Solv Extr Ion Exch 1999, 17, 149–162.
6. Remoudaki, E.; Tsezos, M.; Hatzikioseyian, A.; Karakoussis, V. Biohydrometallurgy and the Environment Toward the Mining of the 21st Century; Amils, R.; Ballester, A., Eds.; Elsevier: Amsterdam, The Netherlands, 1999; Part B, pp 449–462.
7. Ruiz, M.; Sastre, A.; Guibal, E. React Funct Polym 2000, 45, 155.
8. Guibal, E.; Larkin, A.; Vincent, T.; Tobin, J. Ind Eng Chem Res 1999, 38, 4011–4022.
9. Kawamura, Y.; Mitsuhashi, M.; Tanibe, H.; Yoshida, H. Ind Eng Chem Res 1993, 32, 386–391.
10. Piron, E.; Accominotti, M.; Domard, Langmuir 1997, 13, 1653–1658.
11. Guibal, E.; Milot, C.; Tobin, J. M. Ind Eng Chem Res 1998, 37, 1454–1463.
12. Juang, R.-S.; Ju, C.-Y. Acid Ind Eng Chem Res 1998, 37, 3463–3469.
13. Baba, Y.; Hirakawa, H. Chem Lett 1992, 1905–1908.
14. Inoue, K.; Yamaguchi, T.; Iwasaki, M.; Ohto, K.; Yoshizuka, K. Sep Sci Technol 1995, 30, 2477–2489.
15. Wan Ngah, W. S.; Liang, K. H. Ind Eng Chem Res 1999, 38, 1411–1414.
16. Guibal, E.; Vincent, T.; Navarro-Mendoza, R. J Appl Polym Sci 2000, 75, 119–134.
17. Hsien, T. Y.; Rorrer, G. L. Ind Eng Chem Res 1997, 36, 3631–3638.
18. Tien, C. Adsorption Calculations and Modeling; Butterworth–Heinemann: Boston, 1994.
19. Fernandez, M. A.; Laughinghouse, W. S.; Carta, G. J Chromatogr A 1996, 746, 185–198.
20. Kawamura, Y.; Yoshida, H.; Asai, S.; Tanibe, H. Wat Sci Technol 1997, 35(7), 97–105.
21. Bohart, G. S.; Adams, E. G. J Chem Soc 1920, 42, 523.
22. Hutchins R. A. Chem Eng 1973, Aug., 133–138.
23. Ko, D. C. K.; Porter, J. F.; McKay, G. Ind Eng Chem Res 1999, 38, 4868–4877.
24. Roberts, G. A. F. Chitin Chemistry; MacMillan: London, 1992.
25. Charlot, G. Dosages Absorptiométriques des Eléments Minéraux; Masson: Paris, 1978.
26. Guibal, E.; Jansson-Charrier, M.; Saucedo, I.; Le Cloirec, P. Langmuir 1995, 11, 591–598.
27. Milot, C.; McBrien, J.; Allen, S.; Guibal, E. J Appl Polym Sci 1998, 68, 571–580.
28. Chase, H. A. J Chromatogr A 1984, 297, 179–202.
29. Milot, C. Ph.D. Thesis, Université de Montpellier II, U.S.T.L., France, 1998.
30. Guibal, E.; Milot, C.; Roussy, J. Wat Environ Res 1999, 71(11), 10–17.
31. McKay, G.; Blair, H. S.; Gardner, J. R. J Appl Polym Sci 1984, 29, 1499–1514.
32. Kast, W.; Otten, W. Int Chem Eng 1989, 29, 197–211.
33. Weber, W. J., Jr.; DiGiano, F. A. Process Dynamics in Environmental Systems; Wiley: New York, 1996.
34. Ma, Z.; Whitley, R. D.; Wang, N.-H. L. AIChE J 1996, 42, 1244–1262.
35. Jansson-Charrier, M.; Guibal, E.; Roussy, J.; Surjous, R.; Le Cloirec, P. Wat Sci Technol 1996, 34(10), 169–177.